Finite-Time Altitude and Attitude Tracking of a Tri-Rotor UAV using Modified Super-Twisting Second Order Sliding Mode

Yassine Kali[1], Jorge Rodas[2], Maarouf Saad[1], Khalid Benjelloun[3], Magno Ayala[2] and Raul Gregor[2]

[1]*École de Technologie Supérieure, Quebec University, Montreal, QC H3C 1K3, Canada*
[2]*Laboratory of Power and Control Systems, Facultad de Ingeniería, Universidad Nacional de Asunción, Paraguay*
[3]*A2I Laboratory, Ecole Mohammadia d'Ingénieurs, Mohammed V University, Rabat, Morocco*

Keywords: Altitude Tracking, Attitude Tracking, Finite-time Convergence, Lyapunov, Unmanned Aerial Vehicle, Second Order Sliding Mode, Super-twisting Algorithm, Uncertainties.

Abstract: This paper presents the problem of robust altitude and attitude trajectory tracking of a tri-rotor Unmanned Aerial Vehicle (UAV) based on a finite-time second order sliding mode control algorithm. The chosen algorithm is a modified super-twisting control with double closed-loop feedback regulation that provides fast finite-time convergence even when the system trajectories are far from the sliding surface, robustness against a wide class of uncertainties and disturbances. Moreover, this algorithm eliminates the major disadvantage of the classical sliding mode, the well-known chattering phenomenon. The stability analysis of the closed-loop system and the convergence time are given based on a strong Lyapunov function. To show the effectiveness of the used method, simulation results of different scenarios are presented for the considered tri-rotor UAV.

1 INTRODUCTION

In recent years, control of aerial robots have become a coveted field of research. In fact, Unmanned Aerial Vehicles (UAVs) are increasingly used in numerous applications such as construction, visual inspection, exploration, transportation and others (Nex and Remondino, 2014; Sankaran et al., 2015; Segales et al., 2016; Singh and Frazier, 2018). Apart from the fact that UAVs are highly underactuated systems, as all nonlinear systems, they are suffering from uncertainties due to the variation of the inertia and mass (Yang and Xian, 2017) (e.g.: the case of transportation) and external disturbances due to environmental variations as wind (Pflimlin et al., 2004; Ceccarelli et al., 2007) (e.g.: the case of outdoor scenarios)

In literature, several nonlinear controllers have been designed for the problem of tracking and/or stabilization of UAVs such as feedback linearization (Voos, 2009; Zhou et al., 2010), backstepping (Ahmed et al., 2006; Lee et al., 2013), Sliding Mode Control (SMC) (Runcharoon and Srichatrapimuk, 2013) and others. Among these controllers, the best promising one is SMC which is famous for its insensitivity to a wide class of uncertainties and disturbances, its simplicity of design and its finite-time convergence property (Utkin et al., 1999). SMC uses discontinuous control inputs to force the system trajectories to converge to the user-chosen sliding surface. Nevertheless, to ensure all these good features, the discontinuous signals must be high which cause the chattering phenomenon (Fridman, 2001; Boiko and Fridman, 2005). This phenomenon is considered the major drawback of which SMC suffers from. Consequently, the desired performances might be reduced and the system actuators cannot deal with the chattering frequency and might be degraded.

To solve this problem, many works have been developed and published (Lee et al., 2009; Tseng and Chen, 2010; Besnard et al., 2012; Kali et al., 2015). The most popular one for second order systems is the Second Order Sliding Mode (SOSM) introduced in (Levant, 2003). The concept of SOSM is to make the discontinuous signal acting on the derivative of the control input signal, hence, the control input becomes continuous (Kali et al., 2017b; Kali et al., 2017c).

SOSM has been extensively used for UAVs (Benallegue et al., 2008; Zheng et al., 2014; Davila and Salazar, 2017; Munoz et al., 2017a; Munoz et al., 2017b). However, this method requires some informations (e.g.: first time derivative of the sliding surface) that are often not available for measurements.

Kali, Y., Rodas, J., Saad, M., Benjelloun, K., Ayala, M. and Gregor, R.
Finite-Time Altitude and Attitude Tracking of a Tri-Rotor UAV using Modified Super-Twisting Second Order Sliding Mode.
DOI: 10.5220/0006861904350442
In *Proceedings of the 15th International Conference on Informatics in Control, Automation and Robotics (ICINCO 2018) - Volume 1*, pages 435-442
ISBN: 978-989-758-321-6

As a solution to this limitation, the Super-Twisting Algorithm (STA) has been proposed (Guzmán and Moreno, 2015; González-Hernández et al., 2017b; González-Hernández et al., 2017a; Ibarra and Castillo, 2017; Kali et al., 2017a; Kali et al., 2018a; Kali et al., 2018b). Indeed, apart from that STA ensures robustness, finite-time converge and chattering elimination, it does not require the measurements of the first time derivative of the sliding surface. However, when the system trajectories are far from the selected switching surface, the convergence becomes slow (Moreno, 2014) which is not desirable for fast robotic systems.

In order to improve the convergence speed, a modified STA with double closed-loop feedback regulation has been proposed (Yang and Xian, 2017). The proposed algorithm was tested on a DC servo system. The obtained results were satisfactory in comparison with different proposed STA structures. To the authors' best knowledge, this structure has never been used for a tri-rotor UAV system. In this paper, this algorithm will be derived for the altitude and attitude tracking of an uncertain tri-rotor UAV system.

The rest of this paper is organized into four sections as follows. In the next section, the considered tri-rotor UAV is described and its altitude and attitude model are given. In Section 3, the modified STA with double closed-loop feedback regulation is designed for the problem of altitude and attitude tracking in presence of uncertainties and its stability analysis is proved using the Lyapunov method. In section 4, simulation results on the considered tri-rotor UAV are given to demonstrate the effectiveness of the used STA with double closed-loop feedback regulation. The conclusion is given in the fifth section.

2 TRI-ROTOR UAV MODEL

The considered tri-rotor UAV system is shown in Fig. 1. The main advantage of this kind of UAVs is that they require fewer motors than the other proposed multi-rotors UAV systems such as four-rotors or six-rotors. This advantage allows a reduction in volume, weight and energy consumption. The two rotors placed in the forward part of the tri-rotor rotate in opposite direction with respect to the third rotor placed in the backward part.

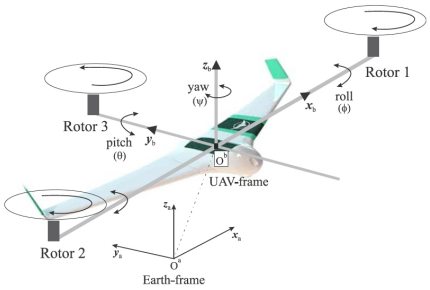

Figure 1: Tri-rotor UAV.

2.1 Altitude Model

The altitude model of the considered tri-rotor can be expressed by the following equation:

$$\ddot{X} = \frac{1}{m}\left(\sin(\psi)\sin(\theta)\cos(\phi) - \cos(\psi)\sin(\phi)\right)\tau_1 \quad (1)$$

$$\ddot{Y} = \frac{1}{m}\left(\cos(\psi)\sin(\theta)\cos(\phi) + \sin(\psi)\sin(\phi)\right)\tau_1 \quad (2)$$

$$\ddot{Z} = -g + \frac{1}{m}\cos(\theta)\cos(\phi)\tau_1 \quad (3)$$

where m denotes the mass of the tri-rotor, g is the constant of gravity, τ_1 is the collective or the vertical force and ϕ, θ, ψ denote the Euler angles (roll ϕ, pitch θ and yaw ψ).

2.2 Attitude Model

The attitude model of the considered tri-rotor can be expressed by the following equation:

$$J W \ddot{\Theta} + J \dot{W} \dot{\Theta} + \left(W \dot{\Theta} \times J W \dot{\Theta}\right) = \tau \quad (4)$$

where $\Theta = [\phi, \theta, \psi]^T$ are the Euler angles, $\tau = [\tau_\phi, \tau_\theta, \tau_\psi]^T$ represents the roll, pitch and yaw torques, $J = \mathrm{diag}(I_x, I_y, I_z)$ is the diagonal inertia matrix while W is the Euler matrix. W and its first-time derivative $\dot{W}$ are defined by:

$$W = \begin{bmatrix} 1 & 0 & -\sin(\theta) \\ 0 & \cos(\phi) & \cos(\theta)\sin(\phi) \\ 0 & -\sin(\phi) & \cos(\theta)\cos(\phi) \end{bmatrix} \quad (5)$$

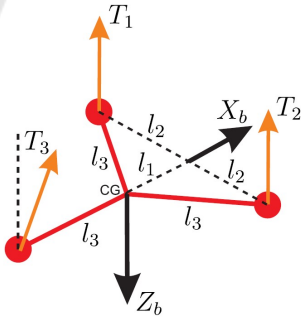

Figure 2: Reference system for the tri-rotor UAV.

Moreover, the control torque inputs can be expressed as follows:

$$\tau_\phi = l_2\left(f_1 - f_2\right) \quad (6)$$

$$\tau_\theta = -l_1\left(f_1 + f_2\right) + l_3 f_3 \cos(\alpha) \quad (7)$$

$$\tau_\psi = -l_3 f_3 \sin(\alpha) \quad (8)$$

$$\tau_1 = f_1 + f_2 + f_3 \cos(\alpha) \quad (9)$$

where α represents the tilting angle of the third rotor placed in the backward part, f_i for $i = 1,2,3$ is the thrust generated by the rotor i, l_i for $i = 1,2,3$ are given in Fig. 2. The control torque inputs given by (6), (7), (8) and (9) can be written in a matrix form as follows:

$$\begin{bmatrix} \tau_1 \\ \tau_\phi \\ \tau_\theta \\ \tau_\psi \end{bmatrix} = \underbrace{\begin{bmatrix} 1 & 1 & \cos(\alpha) \\ l_2 & -l_2 & 0 \\ -l_1 & -l_1 & l_3\cos(\alpha) \\ 0 & 0 & -l_3\sin(\alpha) \end{bmatrix}}_{F} \begin{bmatrix} f_1 \\ f_2 \\ f_3 \end{bmatrix}$$

3 MODIFIED SUPER-TWISTING

In this section, the proposed second order sliding mode controller based on a modified STA for the finite-time altitude and attitude tracking of the considered tri-rotor UAV will be designed. The control objective is to ensure that the altitude and attitude positions defined by Z, ϕ, θ, ψ track with high precision even in presence of uncertainties and disturbances the bounded desired trajectories $Z_d, \phi_d, \theta_d, \psi_d$.

Now, let us introduce $x = [x_1^T, x_2^T]^T$ as state variables with $x_1 = [Z, \phi, \theta, \psi]^T$ and $x_2 = [\dot{Z}, \dot{\phi}, \dot{\theta}, \dot{\psi}]^T$. Then, the equations of motion are given by:

$$\begin{cases} \dot{x}_1 = x_2 \\ \dot{x}_2 = f(x) + g(x)u + h(t) \end{cases} \tag{10}$$

Comparing the above equation with (4) gives the following equivalences:

$$f(x) = \begin{bmatrix} -g \\ -(JW)^{-1}\left(JW\dot{\Theta} + \left(W\Theta \times JW\Theta\right)\right) \end{bmatrix}$$

$$g(x) = \begin{bmatrix} \frac{1}{m}\cos(\theta)\cos(\phi) & 0_{1\times 3} \\ 0_{3\times 1} & (JW)^{-1} \end{bmatrix}$$

$u = \left[\tau_1\, \tau_\phi\, \tau_\theta\, \tau_\psi\right]^T$ and $h(t) \in R^4$ denotes the uncertain vector caused by the wind disturbances, unmodelled dynamics.

In the following, the control law that will force the system trajectories x_1 to track with high accuracy the known desired trajectories $x_{1d} = [Z_d, \phi_d, \theta_d, \psi_d]^T$ is designed based on the following assumptions:

- **Assumption 1:** The system trajectories x_1 and their first-time derivative x_2 are available for measurements.
- **Assumption 2:** The desired trajectories x_{1d} and their first and second time derivatives $x_{2d}, \dot{x}_{2d}$ are known, bounded and limited to:

$$\frac{-\pi}{2} < \phi_d < \frac{\pi}{2},\ \frac{-\pi}{2} < \theta_d < \frac{\pi}{2},\ -\pi < \psi_d < \pi.$$

- **Assumption 3:** The Euler angles (roll, pitch and yaw) are limited to:

$$\frac{-\pi}{2} < \phi < \frac{\pi}{2},\ \frac{-\pi}{2} < \theta < \frac{\pi}{2},\ -\pi < \psi < \pi.$$

Based on all these assumptions, the uncertain functions $h_i(t)$ for $i = 1,2,3,4$ are globally Lipschitz (Derafa et al., 2012):

$$\left|\dot{h}_i(t)\right| \leq \delta_i$$

where $\delta_i > 0$ represents the Lipschitz constant.

Let $e = x_1 - x_{1d} \in R^4$ be the trajectory tracking error. Then, the first step in the design procedure consists on defining the sliding surface. In this paper, the integral sliding surface is selected:

$$S = \dot{e} + K_p\, e + K_I \int_0^t e\, dt \tag{11}$$

where $K_p = \mathrm{diag}(K_{p1}, K_{p2}, K_{p3}, K_{p4})$ and $K_I = \mathrm{diag}(K_{I1}, K_{I2}, K_{I3}, K_{I4})$ are diagonal positive definite matrices. The first time derivative of the above integral sliding surface is computed using the nominal model as follows:

$$\begin{aligned} \dot{S} &= \ddot{e} + K_p\, \dot{e} + K_I\, e \\ &= \dot{x}_2 - \ddot{x}_{1d} + K_p\, \dot{e} + K_I\, e \\ &= f(x) + g(x)\, u - \ddot{x}_{1d} + K_p\, \dot{e} + K_I\, e \end{aligned} \tag{12}$$

Hence, the modified super-twisting control algorithm is obtained by resolving the following equation:

$$\begin{cases} \dot{S} = -K_1\, \Lambda(S)\, \mathrm{sign}(S) - K_2\, S + \varpi \\ \dot{\varpi} = -K_3\, \mathrm{sign}(S) - K_4\, \varpi \end{cases} \tag{13}$$

where $\Lambda(S) = \mathrm{diag}\left(|S_1|^{0.5}, |S_2|^{0.5}, |S_3|^{0.5}, |S_4|^{0.5}\right)$, $K_1 = \mathrm{diag}(K_{11}, \cdots, K_{14})$, $K_2 = \mathrm{diag}(K_{21}, \cdots, K_{24})$, $K_3 = \mathrm{diag}(K_{31}, \cdots, K_{34})$ and $K_4 = \mathrm{diag}(K_{41}, \cdots, K_{44})$ are diagonal positive matrices where the coefficients will be fixed in the stability analysis and $\mathrm{sign}(S) = [\mathrm{sign}(S_1), \mathrm{sign}(S_2), \cdots, \mathrm{sign}(S_4)]^T$ with:

$$\mathrm{sign}(S_i) = \begin{cases} 1, & \text{if } S_i > 0 \\ 0, & \text{if } S_i = 0 \\ -1, & \text{if } S_i < 0 \end{cases} \tag{14}$$

Theorem 3.1. *If the modified STA gains are chosen for $i = 1,2,3,4$ as:*

$$\begin{aligned} &K_{1i} = \gamma K_{3i},\ K_{2i} = \beta K_{4i},\ K_{4i} > 0 \\ &K_{3i} > max\{C1, C2\} \end{aligned} \tag{15}$$

with:

$$\gamma > \frac{|\beta - 2|}{\sqrt{2}\beta},\ \gamma \neq 2,\ \beta > 0,\ \delta_i > 0$$

$$C1 = \frac{\delta_i^2}{\gamma\beta} + \frac{4}{\gamma^3\beta}$$

$$C2 = \frac{32+\gamma^3\beta^2+-8\gamma^2\beta+8\gamma^2\delta_i^2-4\gamma^3\delta_i^2}{4\gamma^3\beta(2-\gamma)}$$

Then, the modified super-twisting control algorithm with double closed-loop feedback regulation for the considered uncertain tri-rotor UAV (10) *is given by:*

$$u = -g(x)^{-1}\left[f(x)+v\right] \tag{16}$$

where v is defined as:

$$\begin{aligned} v = &-\ddot{x}_{1d} + K_p\,\dot{e} + K_I\,e + K_1\,\Lambda(S)\,\mathrm{sign}(S) + K_2\,S \\ &+ K_3\int_0^t \mathrm{sign}(S)\,dt - K_4\int_0^t \varpi dt \end{aligned} \tag{17}$$

ensures finite-time altitude and attitude trajectory tracking.

Proof. The stability of the closed loop error will be analyzed using the same methodology used in (Guzmán and Moreno, 2015). First of all, substituting the modified super-twisting control algorithm (16) in the equation of motion (10) leads to:

$$\begin{aligned} \dot{S} &= -K_1\,\Lambda(S)\,\mathrm{sign}(S) - K_2\,S + \varpi \\ \dot{\varpi} &= -K_3\,\mathrm{sign}(S) - K_4\,\varpi + \dot{h}(t) \end{aligned} \tag{18}$$

The above closed-loop error dynamics can be decomposed into 4 sub-systems as:

$$\begin{aligned} \dot{S}_i(t) &= -K_{1i}|S_i|^{0.5}\,\mathrm{sign}(S_i) - K_2\,S_i + \varpi_i \\ \dot{\varpi}_i &= -K_{3i}\,\mathrm{sign}(S_i) - K_{4i}\,\varpi_i + \dot{h}_i(t). \end{aligned} \tag{19}$$

Now, let us consider the following candidate positive definite Lyapunov function:

$$V = \xi^T L \xi \tag{20}$$

where $\xi = [\xi_{1i}\ \xi_{2i}]^T$ with $\xi_{1i} = |S_i|^{0.5}\mathrm{sign}(S_i)$ and $\xi_{2i} = \varpi_i$ and L is a symmetric positive definite matrix. The Lyapunov function in (20) is positive definite, continuous and differentiable except when the sliding surface is equal to zero $S_i = 0$ and radially bounded by choosing appropriate matrix L as:

$$L = \begin{bmatrix} \beta + \left(\frac{2}{\gamma}\right)^2 & -\frac{2}{\gamma} \\ -\frac{2}{\gamma} & 1 \end{bmatrix} \tag{21}$$

where $\gamma > 0$ and $\beta > 0$. To calculate the first-time derivative of the Lyapunov function, we need to calculate first the first-time derivative of the vector ξ. Remark that $|\xi_{1i}| = |S_i|^{0.5}$. Then, $\dot{\xi} = [\dot{\xi}_{1i}, \dot{\xi}_{2i}]^T$ is as follows:

$$\dot{\xi}_{1i} = \frac{1}{2|S_i|^{0.5}}\dot{S}_i, \ \text{ and } \ \dot{\xi}_{2i} = \dot{\varpi}_i. \tag{22}$$

Hence:

$$\dot{\xi} = \frac{1}{|\xi_{1i}|}A\xi + \frac{1}{|\xi_{1i}|}B\dot{h}_i(t)|\xi_{1i}| \tag{23}$$

where:

$$A = \begin{bmatrix} -\frac{1}{2}\left(K_{1i}+K_{2i}|\xi_{1i}|\right) & \frac{1}{2} \\ -K_{3i} & -K_{4i}|\xi_{1i}| \end{bmatrix}, \quad B = \begin{bmatrix} 0 \\ 1 \end{bmatrix}$$

Moreover, the first time derivative of the Lyapunov function V is calculated as:

$$\dot{V} = \dot{\xi}^T(t)L\xi + \xi^T L\dot{\xi} \tag{24}$$

Substituting $\dot{\xi}$ in $\dot{V}$ leads to:

$$\begin{aligned} \dot{V} &= \frac{1}{|\xi_{1i}|}\xi^T\left(A^TL + LA\right)\xi + \frac{2\dot{h}_i(t)}{|\xi_{1i}|}|\xi_{1i}|B^TL\xi \\ &\leq \frac{1}{|\xi_{1i}|}\xi^T\left(A^TL + LA\right)\xi + \dot{h}_i^2(t)|\xi_{1i}|^2 + \xi^T LBB^TL\xi \\ &\leq \frac{1}{|\xi_{1i}|}\xi^T\left(A^TL + LA + \delta_i^2C^TC + LBB^TL\right)\xi \\ &\leq -\xi^TQ\xi \end{aligned} \tag{25}$$

where $C = [1\,0]^T$. Considering that $K_{1i} = \gamma K_{3i}$ and $K_{2i} = \beta K_{4i}$. Then, Q is calculated as follows:

$$\begin{aligned} Q &= -\frac{1}{|\xi_{1i}|}(A^TL + LA + \delta_i^2C^TC + LBB^TL) \\ &= \begin{bmatrix} Q_{11} & Q_{12} \\ Q_{21} & Q_{22} \end{bmatrix} \end{aligned} \tag{26}$$

where:

$$\begin{aligned} Q_{11} &= \left(\frac{4\beta}{\gamma^2}+\beta^2\right)K_{4i} + \frac{1}{|\xi_{1i}|}\left(\gamma\beta K_{3i} - \delta_i^2 - \frac{4}{\gamma^2}\right) \\ Q_{12} = Q_{21} &= -\left(\frac{2+\beta}{\gamma}\right)K_{4i} + \frac{1}{|\xi_{1i}|}\left(\frac{2}{\gamma} - \frac{\beta}{2}\right) \\ Q_{22} &= 2K_{4i} + \frac{1}{|\xi_{1i}|}\left(\frac{2}{\gamma} - 1\right) \end{aligned}$$

The above matrix Q can be splitted into two matrices as follows:

$$Q = Q_1 + \frac{1}{|\xi_{1i}|}Q_2 \tag{27}$$

where

$$Q_1 = \begin{bmatrix} \left(\frac{4\beta}{\gamma^2}+\beta^2\right)K_{4i} & -\left(\frac{2+\beta}{\gamma}\right)K_{4i} \\ -\left(\frac{2+\beta}{\gamma}\right)K_{4i} & 2K_{4i} \end{bmatrix} \tag{28}$$

$$Q_2 = \begin{bmatrix} \gamma\beta K_{3i} - \delta_i^2 - \frac{4}{\gamma^2} & \frac{2}{\gamma} - \frac{\beta}{2} \\ \frac{2}{\gamma} - \frac{\beta}{2} & \frac{2}{\gamma} - 1 \end{bmatrix} \tag{29}$$

Since Q_1 and Q_2 are symmetrical. Then, they are positive definite if the four following conditions are met:

$$\left(\frac{4\beta}{\gamma^2}+\beta^2\right)K_{4i} > 0 \tag{30}$$

$$\det(Q_1) > 0 \tag{31}$$

$$\alpha\beta K_{3i} - \delta_i^2 - \frac{4}{\gamma^2} > 0 \tag{32}$$

$$\det(Q_2) > 0 \tag{33}$$

The condition in equation (30) is always verified. The inequality in (31) is met if:

$$\gamma > \frac{|\beta - 2|}{\sqrt{2}\beta} \tag{34}$$

While the inequalities in equations (32) and (33) are verified if:

$$K_{3i} > \max\{C1, C2\} \tag{35}$$

with:

$$C1 = \frac{\delta_i^2}{\gamma\beta} + \frac{4}{\gamma^3\beta}$$

$$C2 = \frac{32 + \gamma^3\beta^2 + -8\gamma^2\beta + 8\gamma^2\delta_i^2 - 4\gamma^3\delta_i^2}{4\gamma^3\beta(2-\gamma)}$$

Therefore, verifying the conditions above, $\dot{V}$ is negative definite. Hence, the stability of the closed-loop is proven.

To prove the finite-time convergence, let us recall the fact that the Lyapunov function is radially bounded. Then:

$$\lambda_{\min}\{L\}\|\xi\|_2^2 \leq V \leq \lambda_{\max}\{L\}\|\xi\|_2^2 \tag{36}$$

with $\lambda_{\min}\{L\}$ and $\lambda_{\max}\{L\}$ denote respectively the minimum and maximum eigenvalues of the matrix L and $\|\xi\|_2^2$ is the Euclidean norm of ξ. Hence:

$$\frac{V^{\frac{1}{2}}}{\lambda_{\max}^{\frac{1}{2}}\{L\}} \leq \|\xi\|_2 \leq \frac{V^{\frac{1}{2}}}{\lambda_{\min}^{\frac{1}{2}}\{L\}} \tag{37}$$

In the second part, equation (25) can be rewritten as:

$$\begin{aligned} \dot{V} &\leq -\xi^T Q \xi \\ &\leq -\xi^T Q_1 \xi - \frac{1}{|\xi_{1i}|}\xi^T Q_2 \xi \\ &\leq -\lambda_{\min}\{Q_1\}\|\xi\|_2^2 - \frac{1}{|\xi_{1i}|}\lambda_{\min}\{Q_2\}\|\xi\|_2^2 \end{aligned} \tag{38}$$

where $\lambda_{\min}\{Q_i\}$ is the minimum eigenvalue of Q_i for $i = 1, 2$. As $|\xi_{1i}| \leq \|\xi\|_2$. Then, the above equation can be written as:

$$\dot{V} \leq \frac{\lambda_{\min}\{Q_1\}}{\lambda_{\max}\{L\}}V + \frac{\lambda_{\min}\{Q_2\}\lambda_{\min}^{\frac{1}{2}}\{L\}}{\lambda_{\max}\{L\}}V^{\frac{1}{2}} \tag{39}$$

According to the equation above, the sliding surface converges to zero in finite-time. This concludes the proof.

4 SIMULATION RESULTS

In this section, simulation results are presented in order to demonstrate the effectiveness of the proposed controller based on a modified STA with double closed-loop feedback regulation. The controller is simulated on the altitude and attitude model (10) of the considered tri-rotor UAV described in Section 2 using Matlab/Simulink software. The physical parameters of the used tri-rotor are given in Table 1.

Table 1: Physical parameters of the tri-rotor UAV.

Parameters	Value
Mass, m	2.5 Kg
Nominal mass, $\hat{m}$	2.1 Kg
Moment of inertia, I_x	0.111132 Kg.m^2
Moment of inertia, I_y	0.13282 Kg.m^2
Moment of inertia, I_z	0.249039 Kg.m^2
Nominal moment of inertia, $\hat{I}_x$	0.1 Kg.m^2
Nominal moment of inertia, $\hat{I}_y$	0.1 Kg.m^2
Nominal moment of inertia, $\hat{I}_z$	0.2 Kg.m^2
Length, l_1	0.275 m
Length, l_2	0.42 m
Length, l_3	0.52 m
Gravity, g	9.81 m.s^{-2}

In this part, an altitude and attitude tracking simulation has been performed. The initial altitude positions are chosen to be $X(0) = 0$ m, $Y(0) = 0$ m and $Z(0) = 0$ m while initial Euler angles are chosen to be $\phi(0) = 0$ rad, $\theta(0) = 0$ rad and $\psi(0) = 0$ rad. Moreover, the tracking is performed for the following desired trajectories:

$$Z_d(t) = 10\,\text{m}$$

$$\phi_d(t) = 0.17\sin(\pi t)\,\text{rad}$$

$$\theta_d(t) = -0.17\sin(\pi t)\,\text{rad}$$

$$\psi_d(t) = 0.52\sin(\pi t)\,\text{rad}$$

For this scenario, the chosen controller gains are given in Table 2

Table 2: Modified STA controller gains.

Gains	Value
$K_p = \text{diag}(K_{p1}, \cdots, K_{p4})$	diag(5,5,5,5)
$K_I = \text{diag}(K_{I1}, \cdots, K_{I4})$	diag(6.5,6.5,6.5,6.5)
$K_1 = \gamma K_3$	diag(10,10,10,10)
$K_2 = \beta K_4$	diag(2,2,2,2)
$K_3 = \text{diag}(K_{31}, \cdots, K_{34})$	diag(12,12,12,12)
$K_4 = \text{diag}(K_{41}, \cdots, K_{44})$	diag(1,1,1,1)

The simulation results are given in Figs. 3-8. The proposed modified super-twisting control algorithm ensures the finite-time convergence of the altitude and

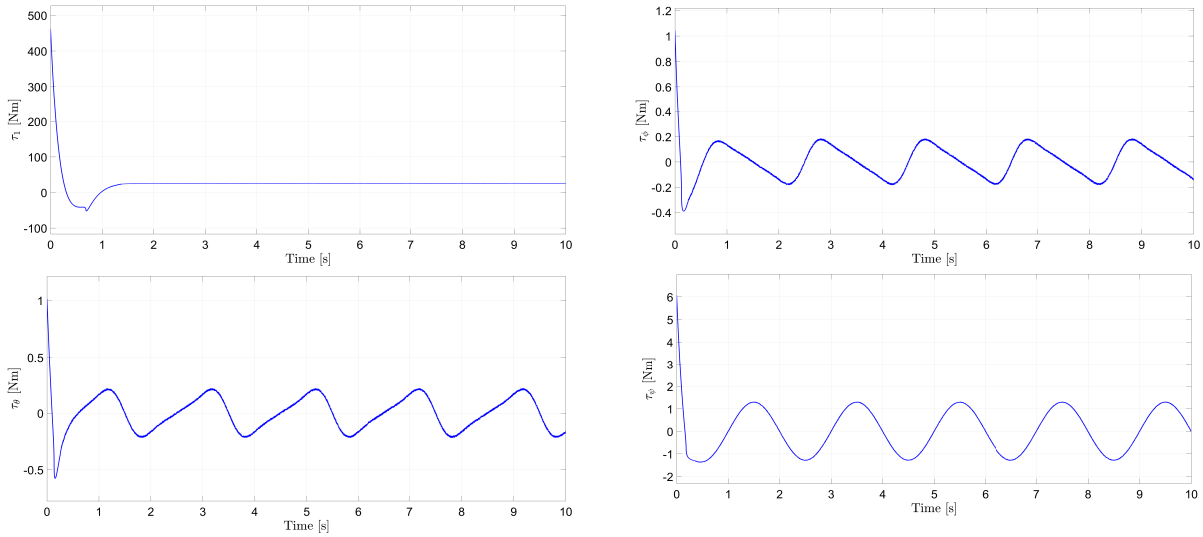

Figure 6: Simulation results of control inputs.

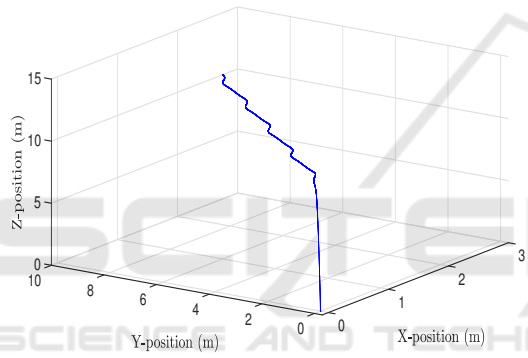

Figure 3: Simulation results of 3D altitude and attitude tracking.

attitude positions to their known desired position trajectories with high precision due to the good rejection of uncertainties and disturbances as shown in Figs. 4 and 7. This is confirmed by the small values of the altitude and attitude tracking error as depicted in Figs. 4 and 8. Moreover, the range of variation of the tilt angle α of the third rotor placed in the backward part in Fig. 5 is fitting the mechanical structure of the system. Figure 6 shows that the control torque inputs effort is very small and chattering free. The values of the control torque inputs are acceptable for our tri-rotor UAV system.

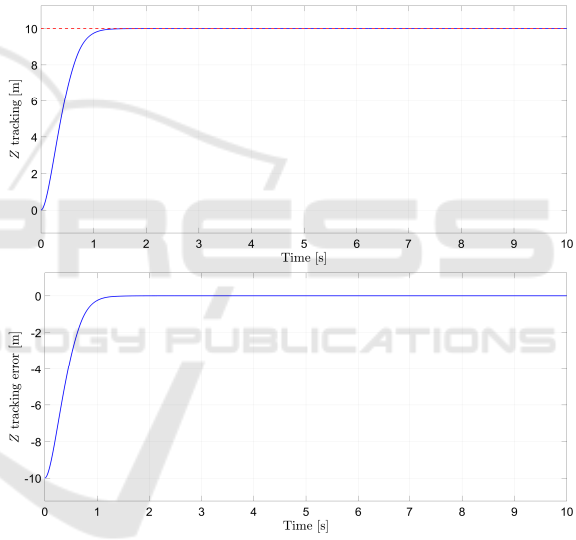

Figure 4: Simulation results of finite-time altitude tracking and tracking error.

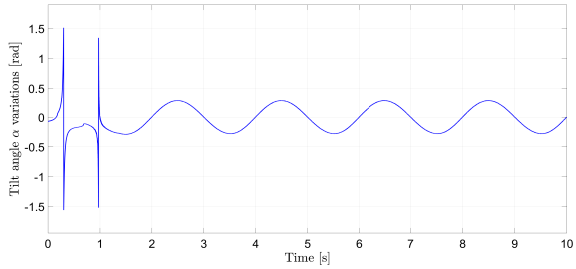

Figure 5: Simulation results of tilt angle variations.

5 CONCLUSIONS

In this paper, a robust modified second order sliding mode control has been designed and successfully simulated on a tri-rotor UAV system for the problem of altitude and attitude tracking in presence of uncertainties and disturbances. The proposed controller ensure robustness by rejecting the effects of the uncertainties and allowing chattering elimination. The obtained simulation results on the considered tri-rotor UAV sy-

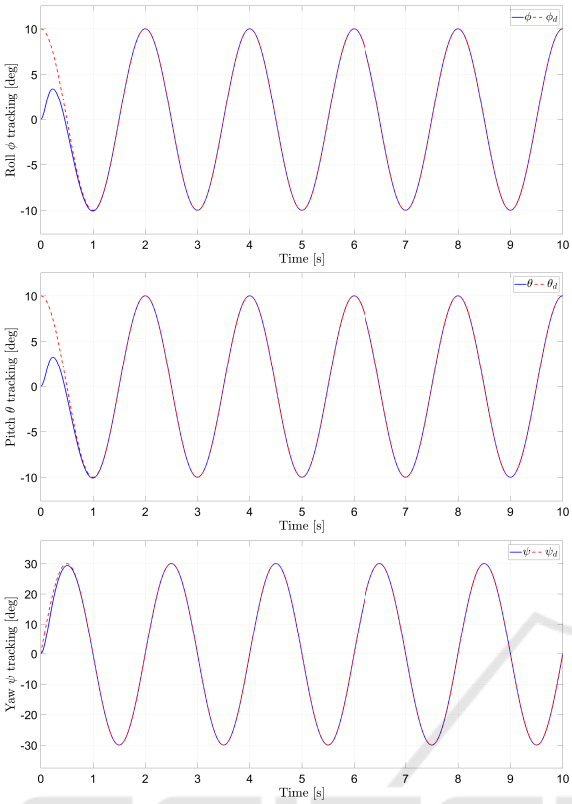

Figure 7: Simulation results of finite-time attitude tracking.

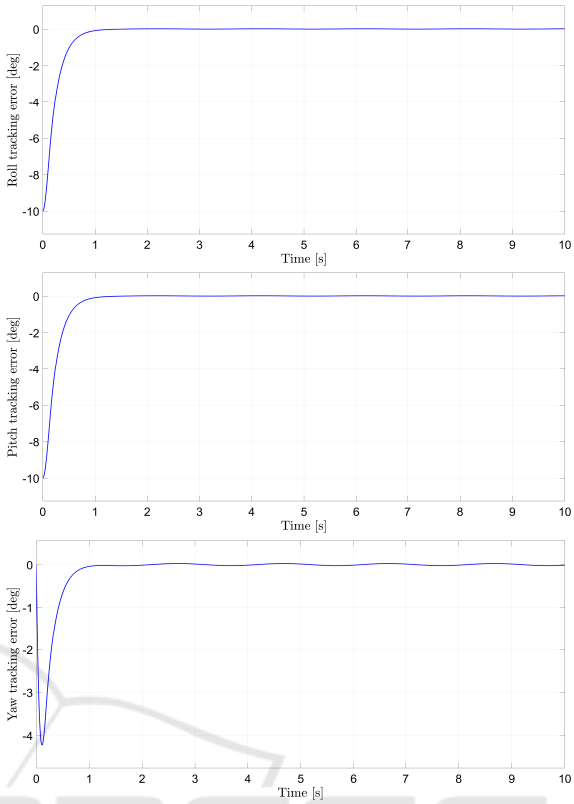

Figure 8: Simulation results of attitude tracking error.

stem show clearly the effectiveness of the proposed modified super-twisting control algorithm in the altitude and attitude tracking and disturbance rejection.

ACKNOWLEDGEMENTS

This work was supported by the Paraguayan Science and Technology National Council - CONACYT (PINV15-0136).

REFERENCES

Ahmed, B., Pota, H. R., and Garratt, M. (2006). Flight control of a rotary wing UAV using backstepping. *International Journal of Robust and Nonlinear Control*, 20(6):639–658.

Benallegue, A., Mokhtari, A., and Fridman, L. (2008). Highorder slidingmode observer for a quadrotor UAV. *International Journal of Robust and Nonlinear Control*, 18(45):427–440.

Besnard, L., Shtessel, Y. B., and Landrum, B. (2012). Quadrotor vehicle control via sliding mode controller driven by sliding mode disturbance observer. *Journal of the Franklin Institute*, 349(2):658 – 684.

Boiko, I. and Fridman, L. (2005). Analysis of chattering in continuous sliding-mode controllers. *IEEE Transactions on Automatic Control*, 50:1442–1446.

Ceccarelli, N., Enright, J. J., Frazzoli, E., Rasmussen, S. J., and Schumacher, C. J. (2007). Micro UAV path planning for reconnaissance in wind. In *ACC, American Control Conference*, pages 5310–5315.

Davila, J. and Salazar, S. (2017). Robust control of an uncertain UAV via high-order sliding mode compensation. *IFAC-PapersOnLine*, 50(1):11553 – 11558.

Derafa, L., Benallegue, A., and Fridman, L. (2012). Super twisting control algorithm for the attitude tracking of a four rotors UAV. *Journal of the Franklin Institute*, 349(2):685 – 699.

Fridman, L. (2001). An averaging approach to chattering. *IEEE Transactions on Automatic Control*, 46:1260–1265.

González-Hernández, I., Palacios, F. M., Cruz, S. S., Quesada, E. S. E., and Leal, R. L. (2017a). Real-time altitude control for a quadrotor helicopter using a super-twisting controller based on high-order sliding mode observer. *International Journal of Advanced Robotic Systems*, 14(1):1–15.

González-Hernández, I., Salazar, S., Munoz, F., and Lozano, R. (2017b). Super-twisting control scheme for a miniature quadrotor aircraft: Application to trajectory-tracking problem. In *ICUAS, International Conference on Unmanned Aircraft Systems*, pages 1547–1554.

Guzmán, E. and Moreno, J. A. (2015). Super-twisting observer for second-order systems with time-varying coefficient. *IET Control Theory Appl.*, 9(4):553–562.

Ibarra, E. and Castillo, P. (2017). Nonlinear super twisting algorithm for UAV attitude stabilization. In *ICUAS, International Conference on Unmanned Aircraft Systems*, pages 640–645.

Kali, Y., Rodas, J., Gregor, R., Saad, M., and Benjelloun, K. (2018a). Attitude tracking of a tri-rotor UAV based on robust sliding mode with time delay estimation. In *ICUAS, International Conference on Unmanned Aircraft Systems*.

Kali, Y., Rodas, J., Saad, M., Gregor, R., Benjelloun, K., and Doval-Gandoy, J. (2017a). Current control based on super-twisting algorithm with time delay estimation for a five-phase induction motor drive. In *IEMDC, IEEE International Electric Machines and Drives Conference*, pages 1–8.

Kali, Y., Saad, M., and Benjelloun, K. (2017b). Non-singular terminal second order sliding mode with time delay estimation for uncertain robot manipulators. In *ICINCO, International Conference on Informatics in Control, Automation and Robotics*, pages 226–232.

Kali, Y., Saad, M., Benjelloun, K., and Benbrahim, M. (2015). Sliding mode with time delay control for mimo nonlinear systems with unknown dynamics. In *2015 International Workshop on Recent Advances in Sliding Modes (RASM)*, pages 1–6.

Kali, Y., Saad, M., Benjelloun, K., and Fatemi, A. (2017c). Discrete-time second order sliding mode with time delay control for uncertain robot manipulators. *Robotics and Autonomous Systems*, 94:53 – 60.

Kali, Y., Saad, M., Benjelloun, K., and Khairallah, C. (2018b). Super-twisting algorithm with time delay estimation for uncertain robot manipulators. *Nonlinear Dynamics*.

Lee, D., Ha, C., and Zuo, Z. (2013). Backstepping control of quadrotor-type UAVs and its application to teleoperation over the internet. In Lee, S., Cho, H., Yoon, K.-J., and Lee, J., editors, *Intelligent Autonomous Systems 12*, pages 217–225, Berlin, Heidelberg. Springer Berlin Heidelberg.

Lee, D., Jin Kim, H., and Sastry, S. (2009). Feedback linearization vs. adaptive sliding mode control for a quadrotor helicopter. *International Journal of Control, Automation and Systems*, 7(3):419–428.

Levant, A. (2003). Higher-order sliding modes, differentiation and output-feedback control. *International Journal of Control*, 76(9-10):924–941.

Moreno, J. A. (2014). On strict Lyapunov functions for some non-homogeneous super-twisting algorithms. *Journal of the Franklin Institute*, 351(4):1902 – 1919.

Munoz, F., Bonilla, M., Espinoza, E. S., González, I., Salazar, S., and Lozano, R. (2017a). Robust trajectory tracking for unmanned aircraft systems using high order sliding mode controllers-observers. In *ICUAS, International Conference on Unmanned Aircraft Systems*, pages 346–352.

Munoz, F., González-Hernández, I., Salazar, S., Espinoza, E. S., and Lozano, R. (2017b). Second order sliding mode controllers for altitude control of a quadrotor uas: Real-time implementation in outdoor environments. *Neurocomputing*, 233:61 – 71.

Nex, F. and Remondino, F. (2014). UAV for 3d mapping applications: a review. *Applied Geomatics*, 6(1):1–15.

Pflimlin, J. M., Soueres, P., and Hamel, T. (2004). Hovering flight stabilization in wind gusts for ducted fan UAV. In *CDC, IEEE Conference on Decision and Control*, volume 4, pages 3491–3496.

Runcharoon, K. and Srichatrapimuk, V. (2013). Sliding mode control of quadrotor. In *TAEECE, International Conference on Technological Advances in Electrical, Electronics and Computer Engineering*, pages 552–557.

Sankaran, S., Khot, L. R., Espinoza, C. Z., Jarolmasjed, S., Sathuvalli, V. R., Vandemark, G. J., Miklas, P. N., Carter, A. H., Pumphrey, M. O., Knowles, N. R., and Pavek, M. J. (2015). Low-altitude, high-resolution aerial imaging systems for row and field crop phenotyping: A review. *European Journal of Agronomy*, 70:112 – 123.

Segales, A., Gregor, R., Rodas, J., Gregor, D., and Toledo, S. (2016). Implementation of a low cost UAV for photogrammetry measurement applications. In *ICUAS, International Conference on Unmanned Aircraft Systems*, pages 926–932.

Singh, K. K. and Frazier, A. E. (2018). A meta-analysis and review of unmanned aircraft system (UAS) imagery for terrestrial applications. *International Journal of Remote Sensing*, 0(0):1–21.

Tseng, M. and Chen, M. (2010). Chattering reduction of sliding mode control by lowpass filtering the control signal. *Asian Journal of Control*, 12(3):392–398.

Utkin, V., Guldner, J., and Shi, J. (1999). *Sliding mode control in electromechanical systems*. Taylor-Francis.

Voos, H. (2009). Nonlinear control of a quadrotor micro-UAV using feedback-linearization. In *ICMA, International Conference on Mechatronics*, pages 1–6.

Yang, S. and Xian, B. (2017). Trajectory tracking control design for the system of a quadrotor UAV with a suspended payload. In *CCC, Chinese Control Conference*, pages 777–782.

Zheng, E.-H., Xiong, J.-J., and Luo, J.-L. (2014). Second order sliding mode control for a quadrotor UAV. *ISA Transactions*, 53(4):1350 – 1356.

Zhou, Q. L., Zhang, Y., Rabbath, C. A., and Theilliol, D. (2010). Design of feedback linearization control and reconfigurable control allocation with application to a quadrotor UAV. In *SysTol, Conference on Control and Fault-Tolerant Systems*, pages 371–376.